micromachines

Article

Time-Modulated Antenna Arrays for Ultra-Wideband 5G Applications

Gonzalo Maldonado [1], Alberto Reyna Maldonado [1], Luz I. Balderas [1,*] and Marco A. Panduro [2]

[1] Electronics Department, Autonomous University of Tamaulipas, UAMRR-R, Carretera San Fernando cruce con Canal Rodhe, Reynosa 88779, Mexico
[2] Electronics and Telecommunications Department, CICESE Research Center, Carretera Ensenada-Tijuana No. 3918, Zona Playitas, Ensenada 22860, Mexico
* Correspondence: luz.balderas@docentes.uat.edu.mx

Abstract: This research presents the design of time-modulated antenna arrays with UWB performance. The antenna arrays consider a linear topology with eight UWB disk-notch patch antennas. The technological problem is to find out the optimum antenna positions and/or time sequences to reduce the side lobes and the sidebands in all of the UWB frequency ranges. The design process is formulated as a bacterial foraging optimization. The results show that the uniform array generates a better SLL performance whereas the non-uniform array obtains a wider bandwidth. The uniform array obtains an SLL < −20 dB from 3.37 GHz to 4.8 GHz and the non-uniform array generates an SLL < −7 dB from 2.97 GHz to 5.26 GHz. The sideband levels are very similar for both cases with a value of around −17 dB.

Keywords: time-modulated array; 4D array; ultrawideband array; G; bacterial foraging optimization

check for updates

Citation: Maldonado, G.; Maldonado, A.R.; Balderas, L.I.; Panduro, M.A. Time-Modulated Antenna Arrays for Ultra-Wideband 5G Applications. *Micromachines* **2022**, *13*, 2233. https://doi.org/10.3390/mi13122233

Academic Editors: Nikola Basta and Milka Potrebic

Received: 23 November 2022
Accepted: 14 December 2022
Published: 16 December 2022

Publisher's Note: MDPI stays neutral with regard to jurisdictional claims in published maps and institutional affiliations.

Copyright: © 2022 by the authors. Licensee MDPI, Basel, Switzerland. This article is an open access article distributed under the terms and conditions of the Creative Commons Attribution (CC BY) license (https://creativecommons.org/licenses/by/4.0/).

1. Introduction

The fifth generation (5G) of wireless communication relies on the use of ultra-wideband (UWB) performance for the internet of things [1]. Particularly, the frequency spectrum from 3 GHz to 5 GHz is very useful for the new communication services in smart cities and manufacturing, health care, and security systems [2]. In the operation of those applications, directive antenna systems such as antenna arrays are commonly required. Traditionally, the antenna arrays are designed by considering the amplitude and phase distributions as element excitations. Nevertheless, one of the emerging design techniques for antenna arrays is the use of time modulation. This technique considers the use of radio frequency switches that turn the antennas on and off over a specific period of time. The main advantage of this technique is the simplification of the beamforming network instead of using amplifiers and phase shifters as traditional arrays. This aspect is very attractive for UWB performance in an antenna array. In this case, the use of time-modulated arrays (TMAs) with UWB performance can be very important for modern applications of 5G. In the field of TMA, there is important research that can be classified as (a) TMA theoretical synthesis and (b) TMA hardware implementation. In TMA synthesis, the synthesis of different array topologies has been reported, such as linear [3,4], square [5,6], circular [7,8], and nonuniform [9–14]. These works were focused on finding the switching time sequences for isotropic sources instead of real antennas. Lately, the performance of TMA has been also studied by utilizing metasurfaces [15–17]. In TMA hardware implementations, there exists important research mainly focused on issues of the implementation of switching time sequences with uniform antenna locations and narrowband performance. For instance, eight dipoles were presented at the central frequency of 2.6 GHz for a uniform TMA in [18–20]. In [21], eight dipoles were also arranged in a uniform array, but at a frequency of 2 GHz. A dual-band TMA with two dipoles was proposed in [22]. This array operates at 2.4 GHz and 5.8 GHz. Moreover,

sixteen printed dipoles were configured in a uniform TMA at 3.25 GHz [23]. Patch antennas have been also used for TMA in a uniform square topology at 5.6 GHz [24].

Recently, the authors from [25] reported a simulated dual-band TMA with nine Vivaldi antennas. Moreover, UWB performance with TMA was theoretically studied in [26]. This paper presented eight Vivaldi antennas forming a simulated uniform linear TMA from 2.65 GHz to 17.26 GHz.

Now, this work proposes two design cases with uniform and non-uniform positions for UWB performance. The research considers the hardware implementation in a linear topology with eight UWB disk-notch patch antennas located in uniform and non-uniform positions. To this end, the design process is formulated as bacterial foraging optimization (BFO) [27]. This algorithm solves the technological problem of finding out the optimum antenna positions and/or time sequences to reduce the side lobes and sidebands in all of the UWB frequency ranges.

2. Time Modulated Array Model

The radiation pattern for a TMA of N elements in the frequency *fr* is formulated by the following mathematical expression [26]:

$$P_{fr}^{m}(\theta, t) = e^{jt(\omega + m\omega_0)} \sum_{n=1}^{N} a_n^m \, g_n^{fr}(\theta) e^{jk(x_n sin\theta cos\varphi)} \tag{1}$$

where

$$a_n^m = \frac{1}{T_0} \int_0^{t_n} w_N\,(t) e^{-jm\omega_0 t}\, dt \tag{2}$$

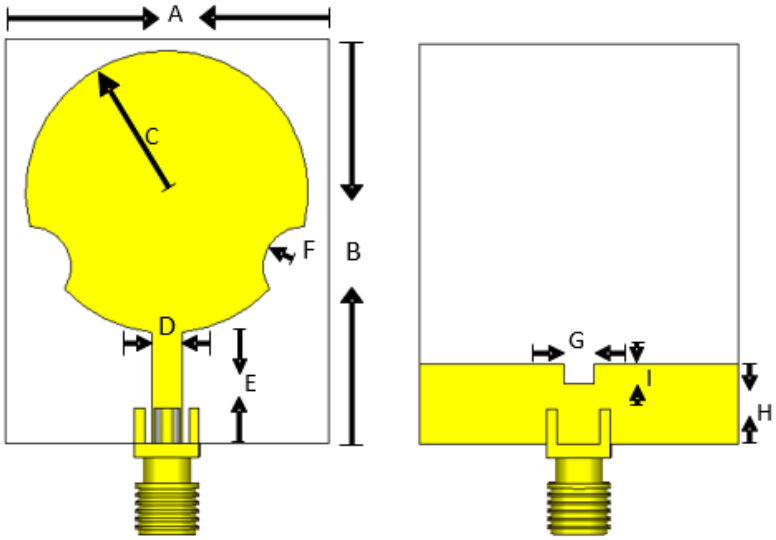
$$w_n(t) = \begin{cases} 1 & for \quad 0 \le t \le t_n \\ 0 & for \quad t_n < t \le T_0 \end{cases} \tag{3}$$

where the terms θ and φ are the elevation and azimuth angles. The wave number is denoted as $k = 2\pi/\lambda$ with λ as the wavelength in the fixed frequency of *fc*. The x_n is the antenna element location on the X-axis from space. This location is measured between the center of the array elements. The terms $\omega = 2\pi f_r$ and $\omega_0 = 2\pi f_0$ are the angular frequency of the RF signal and sidebands, respectively. The T_0 is the period of the periodic function of the time switching function w_n. The term t_n is the time in which the nth UWB disk-notch patch antenna is active in each period. The m represents the number of sidebands. Additionally, the variable a_n^m is the Fourier weight for the sideband m of the antenna n, and the t is the time variable. The function $g_n^{fr}(\theta)$ is the element pattern of the nth antenna in the resonance frequency *fr*. This function considers the mutual coupling phenomena due to the interaction of the remaining elements and the beamforming network. The UWB disk-notch patch antenna is shown in Figure 1 [28].

The UWB element is designed on an FR4 board with a dielectric constant of $\varepsilon_r = 4.3$, a substrate thickness of 1.6 mm with copper metallization of 35 um, a tangential loss value of $\delta = 0.0025$, and an SMA connector. The dimensions of the antenna structure are detailed in Table 1.

Table 1. Antenna Element Dimensions.

A	B	C	D	E	F	G	H	I
32 mm	40 mm	14 mm	3 mm	10.97 mm	4 mm	3 mm	8 mm	2 mm



(**a**) (**b**)

Figure 1. UWB antenna element: (**a**) front view; (**b**) back view.

3. Problem Statement and Optimization Algorithm

The design problem is to discover the optimum locations denoted with x_n and/or time sequences t_n for each element of the TMA to generate optimum radiation patterns in UWB. In this scenario, the optimization variables are defined as:

$$Q = \left[q^1, q^2, q^3, \ldots, q^i\right] \tag{4}$$

$$q^i = \left[x_n^i, t_n^i\right] \tag{5}$$

The Q term is a matrix of optimization variables, and each element q^i represents the x_n and/or the time t_n in which the antenna is turned on. The index term i is an individual from the bacterial population. During the optimization process, the element positions x_n are searched by defining a spacing ($s_n = x_n - x_{n-1}$) among the antennas within the range of $s_n \in [\lambda, 2\lambda]$, where the wavelength λ is considering the lower band of fc = 3.1 GHz, i.e., $s_n \in$ [96.77 mm, 193.54 mm]. This constraint is to avoid a possible overlapping and excessive mutual coupling among the antennas. The time sequences are also constrained such as $t_n \in [0, 1]$. The fitness function of this problem is computed as follows:

$$\mathcal{F}(t_n, x_n) = 50 * \sum_{l=1}^{3} SLL_l + \sum_{l=1}^{3} SBL_l \tag{6}$$

where SLL_l is the maximum side lobe level for the sideband $m = 0$ of the radiation patterns in three (l = 1, 2, 3) different frequencies fr = 3.1 Ghz, fr = 4.1 GHz, and fr = 5 GHz, respectively. The chosen frequencies are in the UWB range where the isolated antenna has a reflection coefficient with a value of $S_{11} < -10$ dB. This term is weighted by a factor of fifty, which was selected by a trial-and-error method. The SBL_l is the maximum value of the sideband $m = 1$ in the above-mentioned frequencies. The algorithm BFO minimizes the function $\mathcal{F}(t_n, x_n)$ to obtain optimum radiation patterns defined in Equation (1) for each frequency. To this end, we follow the methodology of BFO described in [29]. The parameters of the BFO were set up as the number of bacteria S = 25, maximum swimming length N_s = 1, number of chemotactic steps N_c = 5, number of reproduction steps N_{re} = 1000, number of elimination-dispersal events N_{ed} = 1, probability of elimination-dispersion P_{ed} = 0.1, step size $C(i)$ = 0.01 and the number of dimensions that the bacteria can move h = 0.1. This setup has been very efficient for similar optimization problems in [29,30]. We use this algorithm

as an optimization tool for the design; we do not claim that the BFO is the best methodology for this type of design problem.

4. Design Results

The TMA model of Equation (1) and the BFO were implemented in the MATLAB environment. The element patterns $g_n^{fr}(\theta)$ were simulated in the CST software and exported to MATLAB by using a VBA (Visual Basic for Applications) macro. This helps to include the mutual coupling effects in the optimization. The array contains $N = 8$ antennas and the switching period was fixed in $T_0 = 10$ us. We optimized the following design cases: a uniform TMA with element spacing of $\lambda/2$ at the fixed frequency $fc = 3.1$ GHz, and a non-uniform TMA. Table 2 contains the optimum numerical values of the time sequences and antenna locations. These time sequences produce a feed network efficiency of $\eta = 0.7681$ for the uniform array and $\eta = 0.8611$ for the non-uniform array. Figure 2 shows the array of topologies. The uniform array is shorter than the non-uniform array.

Table 2. Optimization Variables.

Variable	Non-Uniform	Uniform Spacing of λ/2
t_n (us)	0.72, 0.9998, 0.9956, 0.9711, 0.6857, 0.96, 0.8334, 0.7169	0.7066, 0.7399, 0.9800, 1.0000, 1.0000, 0.8611, 0.5883, 0.2692
x_n (λ @ 3.1 GHz)	0, 1.3521, 2.3535, 3.76, 5.6241, 6.6395, 8.5758, 10.357	0, 0.5 λ, λ, 1.5 λ, 2 λ, 2.5 λ, 3 λ, 3.5 λ
x_n (mm)	0, 130.76, 227.60, 363.62, 543.89, 642.09, 829.34,1001.60	0, 48.38, 96.77, 145.15, 193.53, 241.91, 290.29, 338.67

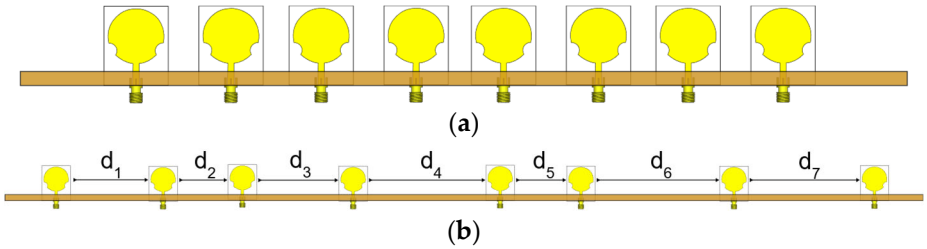


Figure 2. TMA: (**a**) non-uniform; (**b**) uniform spacing of $\lambda/2$.

Figure 3 depicts the reflection coefficients of the active elements at the same time with respect to the reflection coefficient of an isolated antenna, which has an acceptable reflection coefficient from 2.68 GHz to 5.34 GHz. The uniform array reduces the bandwidth because of the closeness of the elements. This array operates from 3.37 GHz to 4.8 GHz. One possible solution to not lose much bandwidth is to increase the spacing of the antennas. The antennas were separated more than a λ. This spacing reduced the mutual coupling effects. When the elements are not so close among others, the UWB performance is not considerably affected. However, the non-uniform array also reduces the bandwidth, but to a lesser amount. This array obtains the reflection coefficients under -10 dB from 2.97 GHz to 5.26 GHz. Figure 4 shows the simulated radiation patterns in the cut-off $\varphi = 0$ and the frequencies of $fr = 3.4$ GHz and $fr = 4.4$ GHz. The sidebands each display 100 kHz of the frequency with respect to the RF frequency fr. The uniform array obtains a better SLL reduction in SLL < -20 dB. The non-uniform TMA generates a lower SLL reduction. Although the minimum spacing is a λ, there are no grating lobes. The non-uniform array produces an SLL reduction in SLL < -7 dB. The sideband levels are very similar for both cases with a value of around -17 dB.

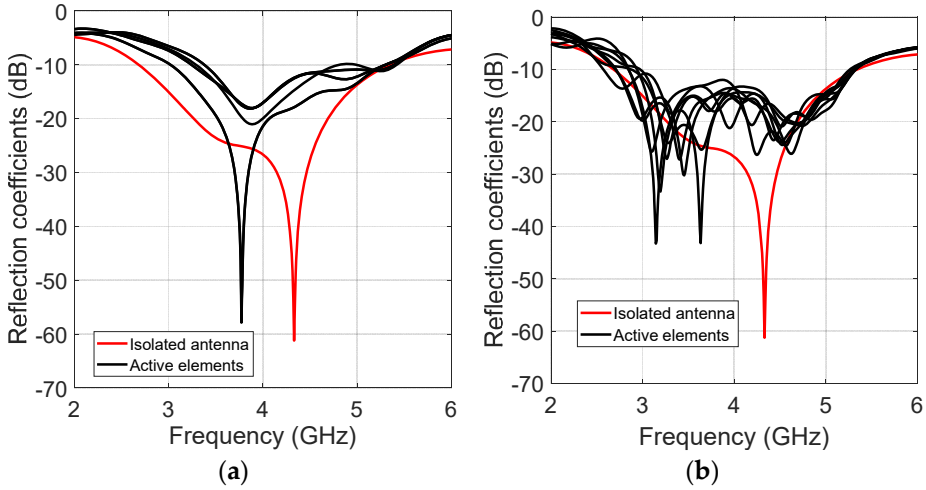


Figure 3. Reflection coefficients: (**a**) uniform spacing $\lambda/2$; (**b**) non-uniform array.

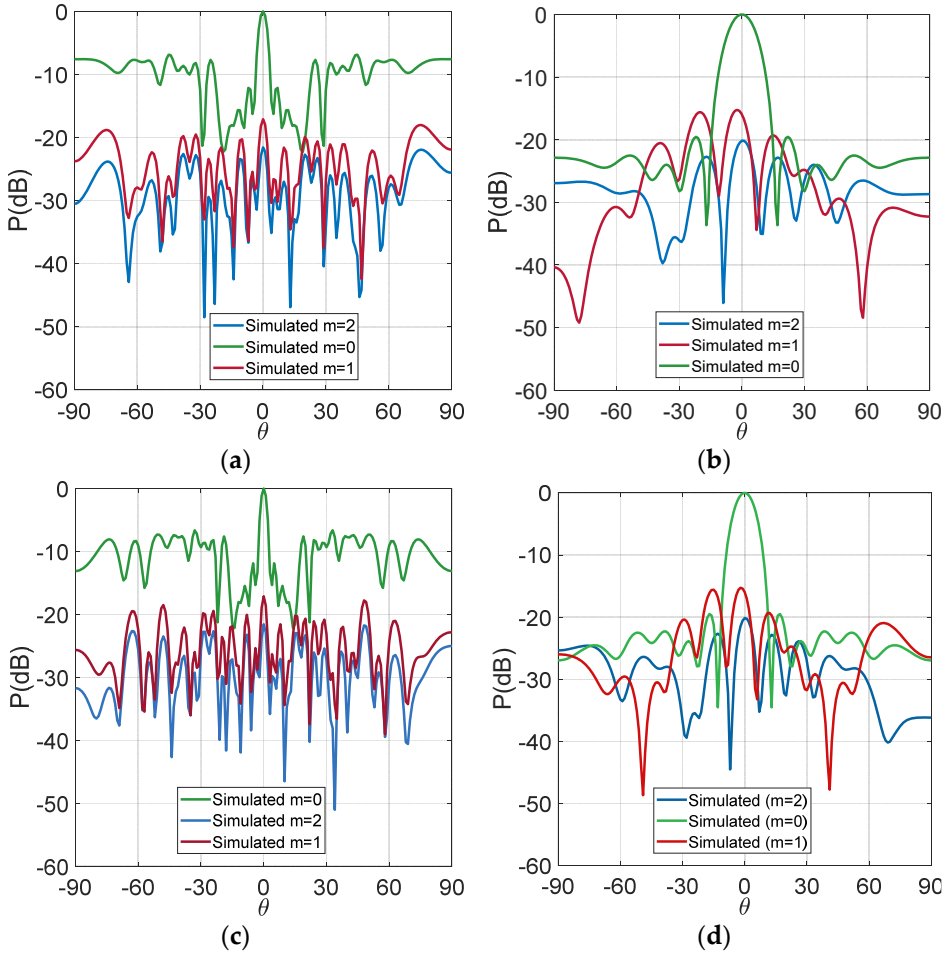


Figure 4. Simulated patterns: (**a**) non-uniform TMA at 3.4 GHz; (**b**) uniform TMA at 3.4 GHz; (**c**) non-uniform TMA at 4.4 GHz; (**d**) non-uniform TMA at 4.4 GHz.

The arrays were fabricated by using eight Mini-Circuits ZFSWA2R-63DR+ switches. Moreover, the firmware was developed for the time modulation on a Digilent FPGA Basys 3. In the beamforming, a Sigatek SP14855 was also used as a power divider. Figure 5 shows a block diagram of the prototypes. The items are connected with RF cables and a pin-header to the SMA connector interface.

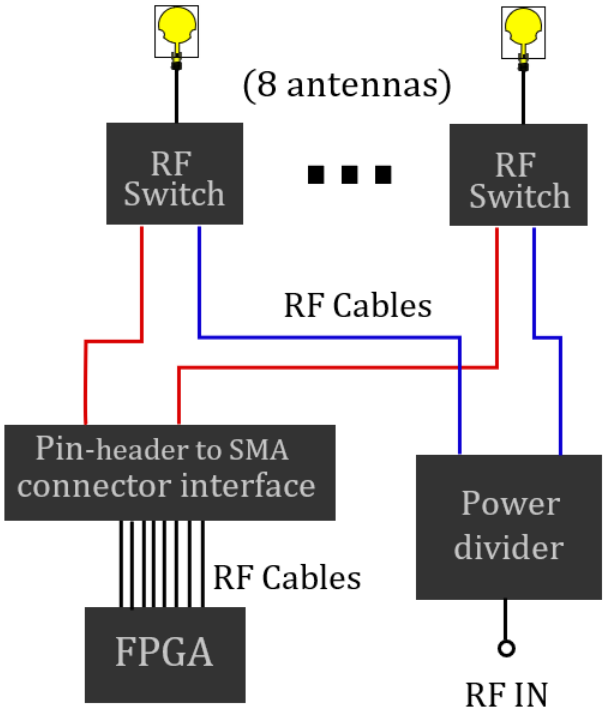


Figure 5. Block diagram of time-modulated arrays.

As is well-known, traditional radiation pattern measurements can be made by an VNA in an anechoic chamber environment. Nevertheless, in TMA technology, this is not feasible because the antennas are momentarily disconnected from the beamforming. This situation complicates the work of the VNA when it tries to capture the S_{21} parameter over a frequency range. As a solution, we alternatively implement the array measurement with the method described in [31,32]. This technique uses a spectrum analyzer to visualize the sidebands versus the frequency inside the anechoic chamber. The spectrum analyzer model Rohde & Schwarz FSV40 was used in the measurements. A broadband horn antenna model ETS-Lindgren 3164-08 was used to send the signals inside the anechoic chamber. The arrays were aligned to the reference antenna and moved very slowly in steps of one degree. Two RF signals were sent to the array to observe the UWB performance. In this case, Figure 6 shows these measured patterns at 3.4 GHz and 4.4 GHz, which are two samples of the UWB frequency range. In the two samples of frequency patterns, a good similarity of SLL with respect to the simulated patterns is achieved.

The sideband level reduction appears as SBL < −17 dB. Figure 7 contains the representation of directivity and SLL versus frequency. We extracted the data of directivity and side-lobe level from different radiation patterns. The frequency range was established from fr = 2.97 GHz to fr = 5.26 GHz in steps of 0.2 GHz. Particularly, Figure 6a presents the simulated directivity of the design cases, the non-uniform array obtains an average of around 11 dB, and the directivity of the uniform array varies from 12 dB to 14.5 dB in the UWB range. Figure 6b illustrates the SLL performance, the SLL for the uniform array is on average −21 dB, and the SLL for the non-uniform array is around −7 dB in all of the UWB frequency ranges.

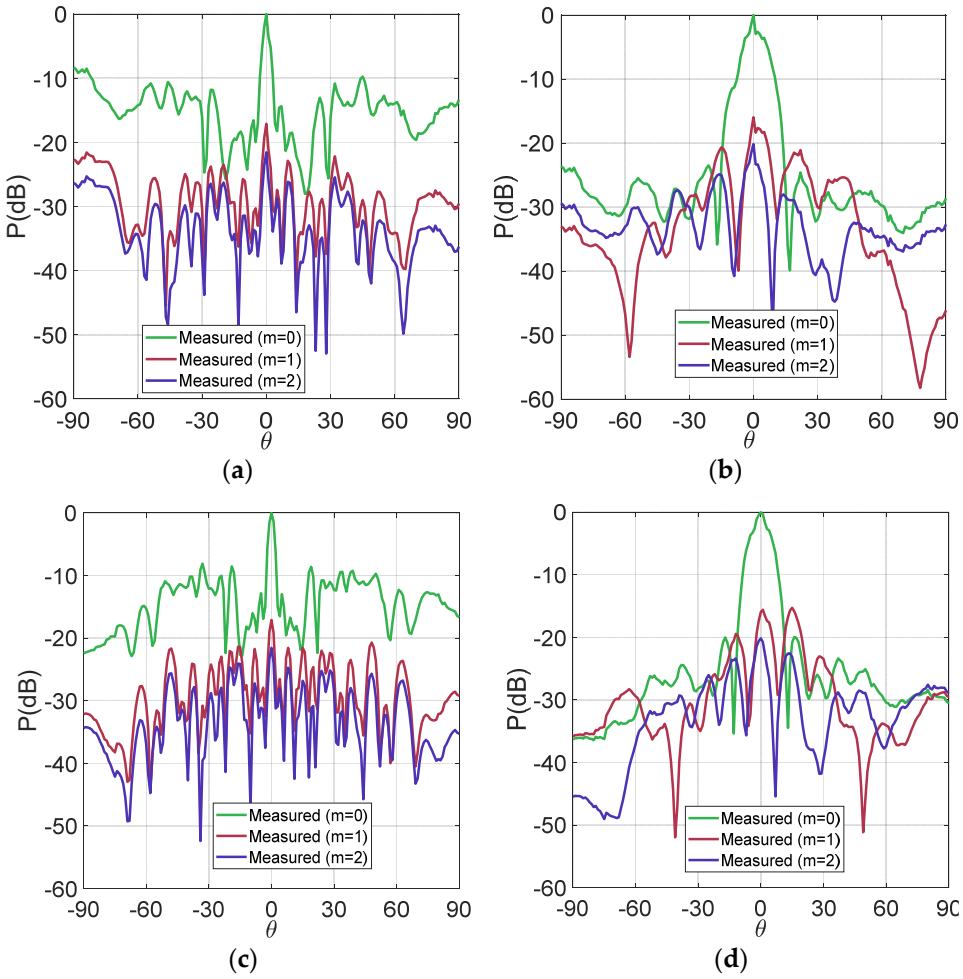


Figure 6. Measured patterns: (**a**) non-uniform TMA at 3.4 GHz; (**b**) uniform TMA at 3.4 GHz; (**c**) non-uniform TMA at 4.4 GHz; (**d**) non-uniform TMA at 4.4 GHz.

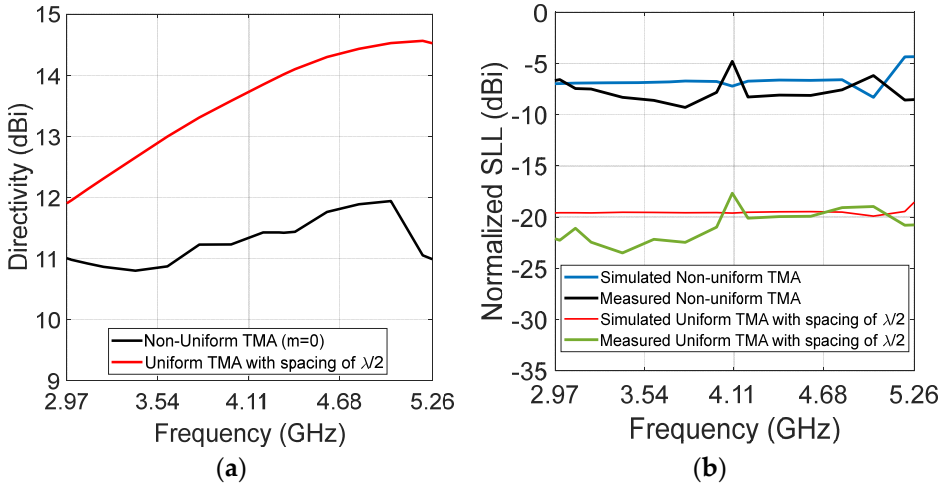
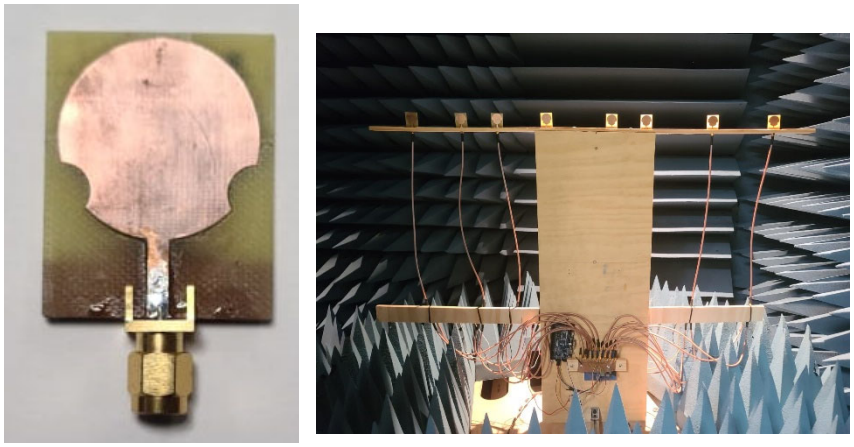


Figure 7. Array performance: (**a**) directivity; (**b**) normalized SLL.

Figure 8 illustrates two photos of one implemented prototype. It shows the fabricated element and the complete non-uniform array under the test. All of the hardware was mounted in a wooden base inside the anechoic chamber.



(**a**) (**b**)

Figure 8. Prototype design: (**a**) single antenna element; (**b**) non-uniform array.

Finally, Table 3 shows a characteristics summary of the designs reported in the literature of TMA and the proposed design. It is highlighted that most of the previous investigations are mainly focused on TMA with narrowband performance and uniform topologies. On the other hand, the research of [25,26] presented only simulations of dual-band and UWB performance of Vivaldi antennas. These arrays also use the uniform spatial distribution of the elements and different time sequences for each frequency. Here, the main contribution of this new research is the use of uniform and non-uniform positions of UWB antennas and only one-time sequence distribution in fabricated TMAs. The utilized frequency range is very suitable for emerging 5G systems.

Table 3. Antenna Array Comparison.

Design	N-Antenna	Freq. (GHz)	Size (mm)	Material	Switch	SLL (dB)	SBL (dB)
Uniform linear [22]	2-Dipole	2.45 and 5.8	136 × 37	FR4	Pin diode BAR63-02	−7.1 and −7.68, for each frequency	−26.28 and −24.53
Uniform linear [21]	8-Dipole	2	525	R4003	AS179-92LF	−11.25	−16.9
Uniform linear [18]	8-Dipole	2.6	403.8	Not provided	Not provided	Not provided	Not provided
Uniform linear [19]	8-Square patch	2.6	403.8	FR4	MAPS-010144-TR0500	Not provided	Not provided
Uniform linear [20]	8-Dipole	2.6	403.8	FR4	Not provided	−22	−25
Uniform square [24]	16-Square patch	5.6	Not provided	Not provided	ADRF5020	14	14
Uniform linear [25]	9-Vivaldi	3.3 and 9.9	121.2	Not provided	Not provided	−18.8	−16.8
Uniform linear [26]	8-Vivaldi	2.65 to 17.26	205.8	FR4	Not provided	−44.95 and −27.88, for each frequency	−14.41 and −14.09
Uniform linear [23]	16-Dipole	3.25	692.3	Not provided	Not provided	−29.1	−28
Nonuniform linear (this work)	8-Disk notch Patch	2.97 to 5.26	1032	FR4	ZFSWA2R-63DR+	−7 (average value)	−17 (average value)
Uniform linear (this work)	8-Disk notch Patch	3.37 to 4.8	38.5	FR4	ZFSWA2R-63DR+	−21 (average value)	−17 (average value)

5. Conclusions

This research presented the feasibility of the implementation of TMA technology with UWB performance. The proposed design was fabricated and measured with eight elements in uniform and non-uniform locations. It obtained good results in terms of SLL and SBL. These arrays can be utilized in emerging 5G systems. The arrays can be also configured

with different amounts and types of UWB antennas to reduce the final size. This will depend on each system. Future works will be focused on the design of a similar array with steering beam capabilities.

Author Contributions: Conceptualization, L.I.B., A.R.M. and G.M.; methodology, G.M. and L.I.B.; software, G.M. and A.R.M.; validation, M.A.P., A.R.M. and G.M.; formal analysis, G.M. and L.I.B.; investigation, G.M.; resources, L.I.B. and A.R.M.; data curation, M.A.P.; writing—original draft preparation, G.M. and A.R.M.; writing—review and editing, L.I.B.; visualization, L.I.B.; supervision, M.A.P.; project administration, L.I.B. and A.R.M.; funding acquisition, M.A.P. and A.R.M. All authors have read and agreed to the published version of the manuscript.

Funding: The research work presented in this paper has been supported by the CONACYT under the grant number 785782 and by UAT with the project number PEI2018-UAT-2022.

Data Availability Statement: Not applicable.

Conflicts of Interest: The authors declare no conflict of interest.

References

1. Johannsen, N.L.; Peitzmeier, N.; Hoeher, P.A.; Manteuffel, D. On the Feasibility of Multi-Mode Antennas in UWB and IoT Applications below 10 GHz. *IEEE Commun. Mag.* **2020**, *58*, 69–75. [CrossRef]
2. Chettri, L.; Bera, R. A Comprehensive Survey on Internet of Things (IoT) Toward 5G Wireless Systems. *IEEE Internet Things J.* **2020**, *7*, 16–32. [CrossRef]
3. Yang, S.; Gan, Y.B.; Qing, A. Sideband suppression in time-modulated linear arrays by the differential evolution algorithm. *IEEE Antennas Wirel. Propag. Lett.* **2002**, *1*, 173–175. [CrossRef]
4. Poli, L.; Rocca, P.; Oliveri, G.; Massa, A. Harmonic Beamforming in Time-Modulated Linear Arrays. *IEEE Trans. Antennas Propag.* **2011**, *59*, 2538–2545. [CrossRef]
5. Capolino, F.; Felsen, L.B. Time Domain Green's Function for an Infinite Sequentially Excited Periodic Planar Array of Dipoles. In Proceedings of the IEEE Antennas and Propagation Society International Symposium, Transmitting Waves of Progress to the Next Millennium. 2000 Digest. Held in Conjunction with: USNC/URSI National Radio Science Meeting (Cat. No.00CH37118). Salt Lake City, UT, USA, 16–21 July 2000; pp. 2054–2057. [CrossRef]
6. Zhu, Q.; Yang, S.; Huang, M.; Nie, Z. Synthesis of low sidelobe time modulated planar arrays with uniform amplitude and sub-sectional optimized time steps. In Proceedings of the 2011 Cross Strait Quad-Regional Radio Science and Wireless Technology Conference, Harbin, China, 26–30 July 2011; pp. 498–501. [CrossRef]
7. Yang, J.; Li, W.T.; Shi, X.W.; Ren, Z. Artificial bee colony algorithm for time-modulated circular antenna array synthesis. In Proceedings of the 2012 International Conference on Microwave and Millimeter Wave Technology (ICMMT), Shenzhen, China, 5–8 May 2012; pp. 1–4. [CrossRef]
8. Guney, K.; Basbug, S. Null Synthesis of Time-Modulated Circular Antenna Arrays Using an Improved Differential Evolution Algorithm. *IEEE Antennas Wirel. Propag. Lett.* **2013**, *12*, 817–820. [CrossRef]
9. Mandal, S.; Kumar Mandal, S. A Comparative Analysis of Power Losses in Time-Modulated Arrays with Uniform, Non-Uniform and Optimized Time-Modulation. In Proceedings of the 2019 International Workshop on Antenna Technology (IWAT), Miami, FL, USA, 3–6 March 2019; pp. 206–209. [CrossRef]
10. Mukherjee, A.; Mandal, S.K.; Ghatak, R. Differential evolution to synthesize low sidelobe thinned isophoric time-modulated planar array with increased directivity. *Int. J. RF Microw. Comput.-Aided Eng.* **2019**, *29*, e21938. [CrossRef]
11. Fondevila, J.; Bregains, J.C.; Ares, F.; Moreno, E. Optimizing uniformly excited linear arrays through time modulation. *IEEE Antennas Wirel. Propag. Lett.* **2004**, *3*, 298–301. [CrossRef]
12. Aksoy, E.; Afacan, E. Thinned Nonuniform Amplitude Time-Modulated Linear Arrays. *IEEE Antennas Wirel. Propag. Lett.* **2010**, *9*, 514–517. [CrossRef]
13. Oraizi, H.; Fallahpour, M. Sum, Difference and Shaped Beam Pattern Synthesis by Non-Uniform Spacing and Phase Control. *IEEE Trans. Antennas Propag.* **2011**, *59*, 4505–4511. [CrossRef]
14. Yang, Q.; Gu, P.; Li, M.; Fan, Z.; Chen, R. Synthesis of Nonuniformly Spaced Wideband Linear Arrays with MSM-FOCUSS Algorithm. In Proceedings of the 2018 IEEE International Conference on Computational Electromagnetics (ICCEM), Chengdu, China, 26–28 March 2018; pp. 1–2. [CrossRef]
15. Chen, M.Z.; Tang, W.; Dai, J.Y.; Ke, J.C.; Zhang, L.; Zhang, C.; Yang, J.; Li, L.; Cheng, Q.; Jin, S.; et al. Accurate and broadband manipulations of harmonic amplitudes and phases to reach 256 QAM millimeter-wave wireless communications by time-domain digital coding metasurface. *Natl. Sci. Rev.* **2022**, *9*, nwab134. [CrossRef]
16. Ke, J.C.; Dai, J.Y.; Chen, M.Z.; Wang, L.; Zhang, C.; Tang, W.; Yang, J.; Liu, W.; Li, X.; Lu, Y.; et al. Linear and Nonlinear Polarization Syntheses and Their Programmable Controls based on Anisotropic Time-Domain Digital Coding Metasurface. *Small Struct.* **2021**, *2*, 2000060. [CrossRef]

17. Zhang, C.; Yang, J.; Yang, L.X.; Ke, J.C.; Chen, M.Z.; Cao, W.K.; Chen, M.; Wu, Z.H.; Chen, J.F.; Cheng, Q.; et al. Convolution operations on time-domain digital coding metasurface for beam manipulations of harmonics. *Nanophotonics* **2020**, *9*, 2771–2781. [CrossRef]
18. Wang, Y.; Lin, F.; Tennant, A. Increasing the energy efficiency of time-modulated reflector-arrays using double layer designs. In Proceedings of the 2016 10th European Conference on Antennas and Propagation (EuCAP), Davos, Switzerland, 10–15 April 2016; pp. 1–5. [CrossRef]
19. Bogdan, G.; Yashchyshyn, Y.; Jarzynka, M. Time-Modulated Antenna Array with Lossless Switching Network. *IEEE Antennas Wirel. Propag. Lett.* **2016**, *15*, 1827–1830. [CrossRef]
20. Chen, K.; Yang, S.; Chen, Y.; Qu, S.-W.; Hu, J. Hybrid Directional Modulation and Beamforming for Physical Layer Security Improvement Through 4-D Antenna Arrays. *IEEE Trans. Antennas Propag.* **2021**, *69*, 5903–5912. [CrossRef]
21. Bogdan, G.; Jarzynka, M.; Yashchyshyn, Y. Experimental study of signal reception by means of time-modulated antenna array. In Proceedings of the 2016 21st International Conference on Microwave, Radar and Wireless Communications (MIKON), Krakow, Poland, 9–11 May 2016; pp. 1–4. [CrossRef]
22. Yashchyshyn, Y.; Derzakowski, K.; Bajurko, P.R.; Marczewski, J.; Kozlowski, S. Time-Modulated Reconfigurable Antenna Based on Integrated S-PIN Diodes for mm-Wave Communication Systems. *IEEE Trans. Antennas Propag.* **2015**, *63*, 4121–4131. [CrossRef]
23. Zhu, Q.; Yang, S.; Zheng, L.; Nie, Z. Design of a Low Sidelobe Time Modulated Linear Array with Uniform Amplitude and Sub-Sectional Optimized Time Steps. *IEEE Trans. Antennas Propag.* **2012**, *60*, 4436–4439. [CrossRef]
24. Bogdan, G.; Godziszewski, K.; Yashchyshyn, Y. Time-Modulated Antenna Array for Real-Time Adaptation in Wideband Wireless Systems—Part II: Adaptation Study. *IEEE Trans. Antennas Propag.* **2020**, *68*, 6973–6981. [CrossRef]
25. Mukherjee, A.; Mandal, S.K.; Ghatak, R. A Fractal-Based Time-Modulated Multiband Linear Array for Interband Communication. *IEEE Antennas Wirel. Propag. Lett.* **2022**, *21*, 918–922. [CrossRef]
26. Revna, A.; Balderas, L.I.; Panduro, M.A. 4D Antenna Array of UWB Vivaldi Elements with Low Side Lobes and Harmonic Suppresion. In Proceedings of the 2018 IEEE International Symposium on Antennas and Propagation and USNC/URSI National Radio Science Meeting, Boston, MA, USA, 8–13 July 2018; pp. 1505–1506. [CrossRef]
27. Shiju, R.M.; Venkateswaran, N. Optimization of linear array antenna pattern synthesis using bacterial foraging algorithm. In Proceedings of the 2012 International Conference on Recent Advances in Computing and Software Systems, Chennai, India, 25–27 April 2012; pp. 130–134. [CrossRef]
28. Kumar, N.A.; Gandhi, A.S. Small size planar monopole antenna for high speed UWB applications. In Proceedings of the 2016 Twenty Second National Conference on Communication (NCC), Guwahati, India, 4–6 March 2016; pp. 1–5. [CrossRef]
29. Passino, K.M. Biomimicry of bacterial foraging for distributed optimization and control. *IEEE Control Syst.* **2002**, *22*, 52–67. [CrossRef]
30. Acharya, O.P.; Patnaik, A.; Choudhury, B. Fault finding in antenna arrays using bacteria foraging optimization technique. In Proceedings of the 2011 National Conference on Communications (NCC), Bangalore, India, 28–30 January 2011; pp. 1–5. [CrossRef]
31. Farzaneh, S.; Ozturk, A.K.; Sebak, A.R.; Paknys, R. Antenna-Pattern Measurement Using Spectrum Analyzer for Systems with Frequency Translation [Measurements Corner. *IEEE Antennas Propag. Mag.* **2009**, *51*, 126–131. [CrossRef]
32. Bogdan, G.; Godziszewski, K.; Yashchyshyn, Y. Feasibility of standard instrumentation for radiation pattern measurement of time modulated antenna array. In Proceedings of the 2018 22nd International Microwave and Radar Conference (MIKON), Poznan, Poland, 14–17 May 2018; pp. 420–423. [CrossRef]